Title
Cost, sustainability and surface roughness quality – A comprehensive analysis of products made with personal 3D printers

Authors
Li, Yalun
Linke, Barbara S
Voet, Henning
et al.

Publication Date
2017

DOI
10.1016/j.cirpj.2016.10.001

Cost, sustainability and surface roughness quality –

A comprehensive analysis of products made with personal 3D printers

Yalun Li [a, b], Barbara S. Linke [a], Henning Voet [b], Björn Falk [b], Robert Schmitt [b], Myron Lam[a]

[a] Department of Mechanical and Aerospace Engineering, College of Engineering, University of California Davis, 1 Shields Ave, Davis, USA

[b] Laboratory for Machine Tools and Production Engineering, RWTH Aachen University, Steinbachstraße 19, Aachen, Germany

E-mail:

Yalun Li: yalun.li@rwth-aachen.de

Barbara S. Linke (Corresponding author): bslinke@ucdavis.edu

Henning Voet: Henning.Voet@wzl.rwth-aachen.de

Björn Falk: B.Falk@wzl.rwth-aachen.de

Robert Schmitt: R.Schmitt@wzl.rwth-aachen.de

Myron Lam: myalam@ucdavis.edu

Abstract: Additive Manufacturing (AM), generally also referred to as 3D printing, has gone through vast development in the past 20 years which still continues. In particular, the market segment of personal 3D printers has achieved an average annually growth rate of approximately 170% from 2008 to 2013. The purpose of this research is to identify the best AM process applied in personal printers in terms of cost, sustainability, surface roughness, and human perception, as these aspects are essential for this new thriving market segment's future. In addition, the research investigates which objective roughness parameters are suitable for qualifying subjective perceptions. The primary AM processes, Fused Deposition Modeling, Stereolithography and Polyjet printing are in the focus of this research. Manufacturing costs as well as environmental impact are calculated, five independent roughness parameters (Ra, Rz, Rq, Rsk, and Rku) are measured and the subjective perception of samples is assessed through sensorial analysis. In conclusion, samples manufactured with Polyjet printing have the best subjective quality, but the highest costs and environmental impact. Biplots of roughness parameters versus sensorial ranking indicates a significant correlation between maximum peak-to-valley height Rz and tactile and visual perception, while the kurtosis of the topography height distribution Rku correlated best to the hedonic rank.

Keywords: Additive manufacturing, 3D printing, roughness, hedonic, visuotactile, perception, cost, sustainability, environmental impact

1. Introduction

1.1. Background

Low-cost desktop 3D printers, or personal 3D printers, are those additive manufacturing (AM) machines with a unit price under $5.000 [1]. Though their history is much shorter compared to industrial 3D printers, this market segment has been booming in recent years, with an average annually growth rate of approximately 170% to date from 2008. The amount of personal 3D printers has surpassed industrial printers by several scales in terms of growth rate and quantity [1]. The rapid development of personal 3D printers is mostly based on the Stratasys' Fused Deposition Modeling (FDM®) technology [2] , the first multi-material 3D printer "Fab@Home" [53] and the RepRap open source machine development project [3] since 2007. As a result, a dominant quantity of personal 3D printers is based on Stratasys' patented technology FDM® and Fused Filament Fabrication (FFF) technologies. The American Society for Testing and Materials (ASTM) classifies all of these AM principles as material extrusion technologies, in which material is selectively dispensed through a nozzle or orifice [4].

With the development of the personal 3D printing market segment, few fundamentally new processes have been developed and few existing AM processes have also been reapplied toward the personal 3D printer segment, including Vat Photopolymerization and Material Jetting. Vat Photopolymerization is an AM process in which liquid photopolymer in a vat is selectively cured by light-activated polymerization [4] as Stereolithography Apparatus (SLA®). Polyjet®, as an AM process in which droplets of build material are selectively deposited and cured with UV light [4], is an example for Material Jetting.

1.2. Research objective

A key advantage of AM is the ability to facilitate customized production and allow designs that were not possible with previous manufacturing techniques. With the significant development in previous years, AM technology seems to open up new opportunities for the economy and society. Various challenges, however, can impede and slow the adoption of this technology, to which their cost effectiveness in comparison to traditional manufacturing methods and ability to fulfill the social demand on cleaner production and sustainability belongs. Therefore, the manufacturing cost and environmental impact of these AM processes have to be evaluated.

Besides that, the main application field of personal 3D printers is prototyping. According to statistics collected by 3D Hubs over 10.000 printers, their main applications are categorized as: Prototype, Hobby/DIY, Gadget, Art/Fashion, Scale model and Household [5]. Therefore, in comparison to mechanical or thermal properties, the tactile and visual perception along with aesthetic coordination has more influence on how the consumers assess the quality of 3D printed parts.

Today, the surface quality of plastics manufactured by FDM, SLA, and Polyjet printing and main influencing factors have been comprehensively researched. Previous studies have found that layer thickness and road width[1] have significant influence on FDM parts [6]. Layer thickness, hatch and fill spacing affect the inclined and horizontal planes of SLA parts [7]. In Polyjet parts the layer thickness and built style (matte or glossy) are the most influencing factors [8]. In mutual comparison, FDM parts have the roughest surface [9]. Polyjet printing surpasses SLA in surface quality in all inclined surfaces but not for an inclination of 90°, which is the vertical surface [9].

However, how the printed parts of these processes are perceived by consumers and which parameter will influence their perception has not been investigated yet. Therefore, this research will focus on the most relevant 3D printing processes for plastic parts, FDM, SLA, and Polyjet printing, and investigate which measured surface roughness parameters are suitable for qualifying subjective perceptions. In addition, costs and environmental impacts will be investigated.

[1] Thickness of the road that the FDM nozzle deposits

2. Sample preparation

Several samples were manufactured with different AM techniques to compare cost, environmental impact, roughness and sensory quality. The dimensions of the benchmark samples are 38.1 mm x 38.1 mm x 38.1 mm (1.5” x 1.5” x 1.5”). **Figure 1** shows the sample details.

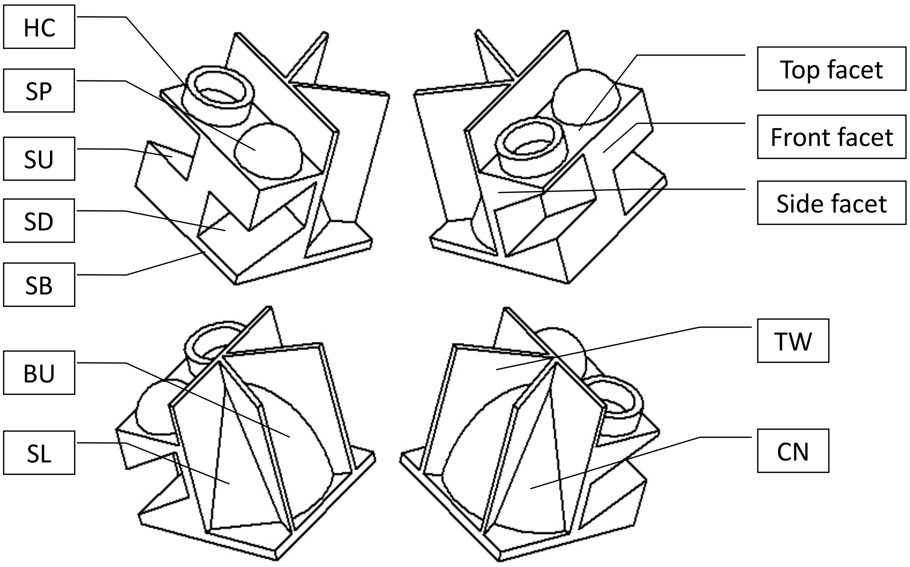

Figure 1 The benchmark part

To achieve a performance evaluation and comprehensive perception by assessors towards 3D printing, the benchmark part includes key shapes and features, which are increasingly required or expected of AM processes and suitable for fabrication in a typical personal 3D printing machine. Similar geometric features are used in a study on AM process comparison including SLA and FDM by Mahesh et al. [10]. The geometric features shown in Figure 2 are identified by two-letter names, such as SB, HC, etc. for referencing in the succeeding table and results. They are also summarized in **Table 1** in alphabetical order.

Table 1 Summary of the sample’s features

Abbreviation	Features	Nominal size
BU	Bullet	Base diameter 17.78 mm (0.7”)
CN	Cones	Base diameter 16.26 mm (0.64”)
HC	Hollow cylinders	Outer diameter 15.24 mm (0.6”) and inner diameter 11.43 mm (0.45”)
SB	Square base	38.1 x 38.1 x 1.27 mm (1.5” x 1.5” x 0.05”)
SD	Slot downwards	Inclination 30° beneath horizontal, slot height 12.7 mm (0.5”)
SL	Slope	Inclination 60° above horizontal
SP	Spheres	Diameter 15.24 mm (0.6”)
SU	Slot upwards	Inclination 30° above horizontal, slot height 12.7 mm (0.5”)
TW	Thin wall	Thickness 1.27 mm (0.05”)

Five samples were chosen for the final assessment. The sample's manufacturing details are listed in **Table 2**.

Table 2 Summary of samples' technical properties

Sample	Machine	AM process	Material	Layer thickness (microns)	Infill density	Color	Weight (g)
I	Makerbot Replicator	FDM	PLA	100	15%	Translucent	15.23
II	Makerbot Replicator 2X	FDM	ABS	100	10%	Black	10.24
III	Formlabs Form 1+	SLA	UV curing resin	50	100%	Translucent	29.01
IV	Stratasys Objet260	Polyjet	VeroClear	32	100%	Translucent	28.46
V	Stratasys Objet260	Polyjet	Digital material	16	100%	Blue	28.93

The chosen materials are the most relevant for each additive manufacturing process: FDM with polylactic acid (PLA) [11] and acrylonitrile butadiene styrene (ABS) [12], SLA with a clear ultra-violet (UV) curing resin [13], Polyjet printing with translucent UV resin VeroClear [14] and Digital material[2] Grey 60 [15]. All materials are provided by the manufacturers of the AM machines used. FDM parts were built with the machine's minimum layer thickness setting of 100 microns for a better benchmarking. Without concern about samples' strength, infill density for FDM parts is chosen at the lowest reasonable level to save print time and material [47]. An infill density lower than 100% is not possible for parts originated from photosensitive materials, because any overhanging features of the parts must be supported during the build process to prevent them from collapsing under their own weight [51] [52]. The sample with a potential structure inside would have a closed shell. This prevents the removal of the supporting uncured resin (at SLA printing) or of the supporting material (at Polyjet printing). For FDM parts their low infill density can significantly reduce own weight, up to approximately one third of SLA and Polyjet samples' weights.

The SLA part was built with the default layer thickness of 50 microns, while the Polyjet part was made with default 32 microns and 16 microns. Furthermore, the FDM and Polyjet parts were built from square bases in the vertical direction, whereas the SLA parts were tilted with a vertical angle according to the recommendation from the used Formlabs' software. The SLA part is presented in **Figure 2**.

[2] Digital Material is composite material with predetermined visual and mechanical properties from Stratasys Inc. [16].

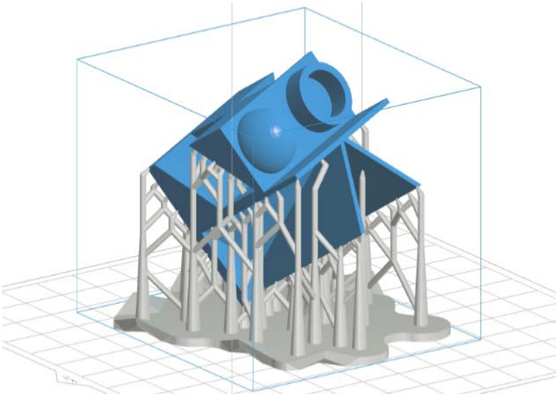

Figure 2 Build direction of SLA sample in printer

To ensure a minimum effect of post-processing on the samples' surface roughness, the post-processing procedures are strictly confined to 1st level procedures as defined in the Wohlers report [17]. These 1st level procedures are the separation of the printed part from surrounding liquids or loose powders and removal of supporting structures without influencing the surface topography. In this research, the supporting structure for the FDM parts at the opening of geometric feature SD were manually removed and finished. The SLA sample was put into isopropanol for several minutes after fabrication. Then the support structures (as seen in Figure 2) were also manually removed and finished. The Polyjet samples were removed from the build platform using a knife and the supporting powders remaining in the geometric features SD and SU were removed with high-pressure water jet in a wash box.

3. Manufacturing costs

According to Son [37], the manufacturing costs for 3D printing can be categorized in two different ways: (1) for "well-structured costs", e.g. labor, material, and machine costs and (2) for "ill-structured costs" involving those associated with build failure, machine setup, and inventory. As the "ill-structured costs" relates more to possibilities for savings in a supply chain, the two major manufacturing costs models for 3D printing by Hopkinson and Dickens [38] and Ruffo et al. [39] are based on the "well-structured costs". The suitable equations for this research's printing scenario and the main assumptions includes: (1) only one part is manufactured in each build, (2) the printer will completely depreciate after eight years and (3) the printer worked 100 hours per week for 50 weeks per year (57 % utilization).

The equation for manufacturing costs C_{sum} in total is as following:

$$C_{sum} = C_{machine} + C_{labor} + C_{material} + C_{energy} \quad (1)$$

$$C_{machine} = \frac{p_{machine}}{t_{dep} * e_u} * t_{man} \quad (2)$$

$$C_{labor} = \frac{s_{labor}}{t_{annual}} * t_{assist} \quad (3)$$

$$C_{material} = C_{direct} + C_{indirect} = p_{material} * m_{material} + p_{support} * m_{support} \quad (4)$$

$$C_{energy} = P_{elec} * p_{electricity} * t_{man} \quad (5)$$

$p_{machine}$: Machine cost

t_{dep}: Duration for machine depreciation (8 years) [38]

e_u: Annual utilization rate (57%)

t_{man}: Manufacturing time for a sample

S_{labor}/t_{annual}: Average salary per hour in UC Davis for lab technician ($15/h) [40]

t_{assist}: Time for assistance for manufacturing's set-up and samples' cleaning (0.5h)

$p_{material}$: Price for build material

$m_{material}$: Weight for build material (including waste)

$p_{support}$: Price for supporting material

$m_{support}$: Weight for supporting material

P_{elec}: Machine Power

$p_{electricity}$: Average electricity price in Davis, CA ($0.1153/kWh) [41]

The costs for facility rent, maintenance, equipment and software (referred to as administrative overhead by Ruffo et al. with 1.4% in total cost) were ignored. All relevant data is listed in **Table 3**. For Polyjet parts secondary gel-like support material was used and its data is shown behind the build material in square brackets.

Table 3 Summary of samples' manufacturing costs related data

Sample	t_{man} (min)	P_{elec} (W)	$p_{machine}$ ($)	$m_{material}$ [$m_{support}$]	$p_{material}$ [$p_{support}$]	$C_{machine}$ ($)	C_{labor} ($)	$C_{material}$ ($)	C_{energy} ($)	C_{sum} ($)	C_{sum}/m_{smp}* ($/g)
I	62	100	2,899	15.8g	$53/kg	0.075	7.5	0.837	0.012	8.424	0.553
II	63	150	2,499	15.8g	$48/kg	0.066	7.5	0.758	0.018	8.342	0.815
III	380	60	3,299	36ml (38.5g)	$149/L	0.523	7.5	5.364	0.044	13.431	0.463
IV	75	1500	120,000	51g [34g]	$333/kg [$130/kg]	3.755	7.5	16.983 [4.42]	0.216	32.874	1.155
V	144	1500	120,000	56g [34g]	$281/kg [$130/kg]	7.210	7.5	15.736 [4.42]	0.415	35.381	1.223

* See sample weights in **Table 2**

As seen in **Table 3**, the Polyjet parts (IV and V) have the significantly highest costs among the three AM processes, whereas FDM parts (I and II) have the lowest. The price for the SLA part (III) is in the middle. Labor costs contribute greatly to manufacturing costs and the effect is more significant with relatively low-cost FDM printers. For cost per weight C_{sum}/m_{smp}, however, the SLA part (III) has the lowest value, followed by FDM parts and Polyjet parts. The cost per weight span only from 0.463 $/g (100%) to 1.223 $/g (about 260%), whereas the total cost span from $8.342 (100%) to $35.381 (about 420%). However, as the Polyjet printers have the ability to manufacture multiple parts within one build without a significant increase in time due to a scan width of 2.5'' by UV lamp, the cost per part could be reduced correspondingly [29] [42]. Because today the material costs of Polyjet printing are considerably higher than total costs for FDM and SLA products, it is not realistic for Polyjet to achieve the same price per unit as FDM or SLA. Multiple printings make Polyjet printing more competitive.

4. Environmental impact of the printed parts

With the maturing of 3D printing techniques, the public considers higher sustainability as a key advantage. It is expected that AM can reduce environmental impact and energy consumption significantly compared to traditional manufacturing practices, such as injection molding of plastics [33] [49]. Many relevant studies were done on AM techniques, but without a specialized focus on personal 3D printers [32] [43] [44]. The following shows two approaches to analyze environmental impacts of the printed parts.

4.1 Evaluation with life-cycle methodology

The first evaluation method to assess the environmental performance of AM processes is based on the work by Luo et al. [43]. As a life cycle methodology it includes environmental impacts in all life cycle stages.

The hierarchical process model by Luo et al. applies Eco-Indicator 95 [46] as Environmental and Resource Management Data (ERMD), which defines ways to quantify the consequences of impairment of the environment. Four AM products' life cycle phases are in focus: (1) raw material preparation, (2) build process, (3) product usage and (4) disposal. In the build process phase the environmental impact of AM per se and possible residues are considered, and in the use phase the material toxicity. Three different methods (recycling, landfill, and incineration) are available for the disposal phase. The entire methodology is shown in **Figure 3**.

The final result of AM products' environmental impact is called environmental performance value (EPV) and its unit is Eco-indicator Point (Pt), which is divided into 1000 millipoints (mPt). The higher the EPV, the more environmental impact an AM product causes. 1 Pt indicates one thousandth of the yearly environmental load of an average citizen in Europe.

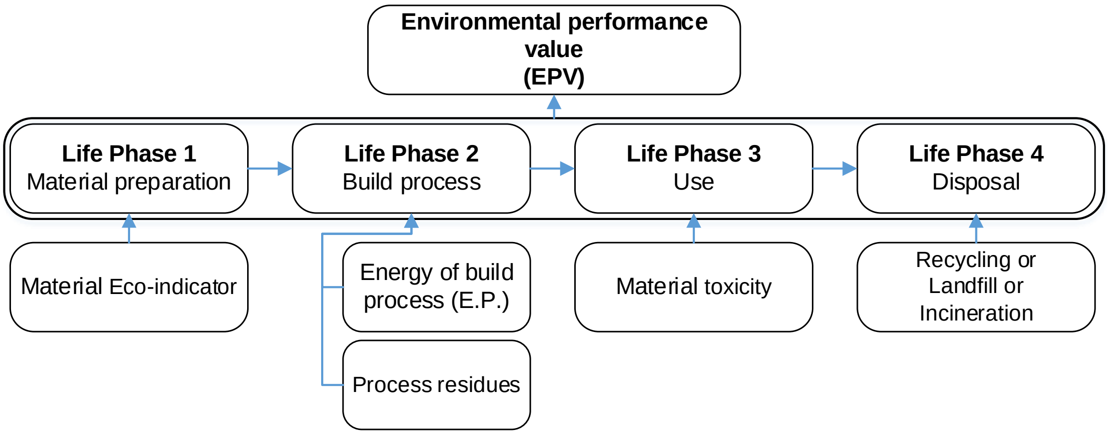

Figure 3 Process model of environmental performance

The following equations calculate the environmental impact of the build processes, which is expressed in Energy in Process (E.P.) and represents the environmental impact of energy used to process one kilogram of print material.

$$E.P. = f_{C_{elec}} \cdot ECR \quad (7)$$

$$ECR = \frac{P}{PP} \quad (8)$$

$$\mathrm{PP} = V * W * T * \rho * k \quad (9)$$

or simplified

$$\mathrm{PP} = m_{smp}/t_{man} \quad (10)$$

ECR: The energy use during the process (kWh/kg)

$f_{C_{elec}}$: A factor in Eco-Indicator 95 to convert ECR to an environmental impact expressed in mPt/kg (0.57 mPt/kWh) [46]

P: Machine power rate

PP: The process productivity (kg/h)

V: Scanning (drawing) speed (mm/sec)

W: Road width size (mm)

T: Layer thickness (mm)

ρ: Material density (kg/cm^3)

k: Process overhead coefficient (0.6-0.9) [43]

m_{smp}: Input material weight (see Table 3)

t_{man}: Manufacturing time for a sample

The processes' E.P. is analyses as summarized as following in **Table 4**. It can be seen from the final result of $E.P.$ that the build process of sample V causes 17 times more environmental impact than sample I.

Table 4 Summary of build processes' environmental impact related data

Sample	Machine	t_{man} (min)	V (mm/s)	W (mm)	T (mm)	ρ (g/cm^3)	k	PP (g/h)	P (kW)	ECR (kWh/kg)	E.P. (mPt/kg)
I	Replicator	62	85	0.4	0.1	1.25	0.9	13.77	0.1	7.25	4.13
II	Replic. 2X	63	85	0.4	0.1	1.07	0.9	11.79	0.15	12.71	7.24
III	Form 1+	380	90	0.3	0.05	1.15	0.7	3.91	0.06	15.35	8.75
IV	Objet260	75	N/A	N/A	0.032	1.18	0.6	68,00*	1.5	22,06	12.57
V	Objet260	144	N/A	N/A	0.016	1.17	0.6	37,50*	1.5	40,00	22.80

*Calculated with equation (10)

Table 5 shows the samples' EPV as total value of 4 life cycle phases (**Figure 3**). The EPV was calculated in the left row for 1kg of input material, then in the right row according to input material for the manufacturing of one sample. In disposal phase the method with least environmental impact was chosen. The data refers to Eco-indicator 95 [46].

Table 5 Environmental performance value of the samples

Sample	Raw Material (mPt)	Build process (mPt)		Use (mPt)	Disposal (mPt)			Total EPV (mPt)	
	Eco-indicator	E.P.	Process residues	Material toxicity	Recycling	Landfill	Incineration	Per 1 kg	Used Material
I	13	4.13	negligible	0	-5	0.035	1.8	12.13	0.19
II	9.3	7.24	negligible	0	-5	0.035	1.8	11.54	0.18
III	10	8.75	negligible	1.2	N/A	0.035	1.8	19.98	0.77
IV	10	12.57	negligible	1.2	N/A	0.035	1.8	23.81	2.02
V	10	22.80	negligible	1.2	N/A	0.035	1.8	34.04	3.06

* See used material weights in **Table 3**

The results of total EPV of used material for samples and their distribution in different life phases are illustrated in **Figure 4**.

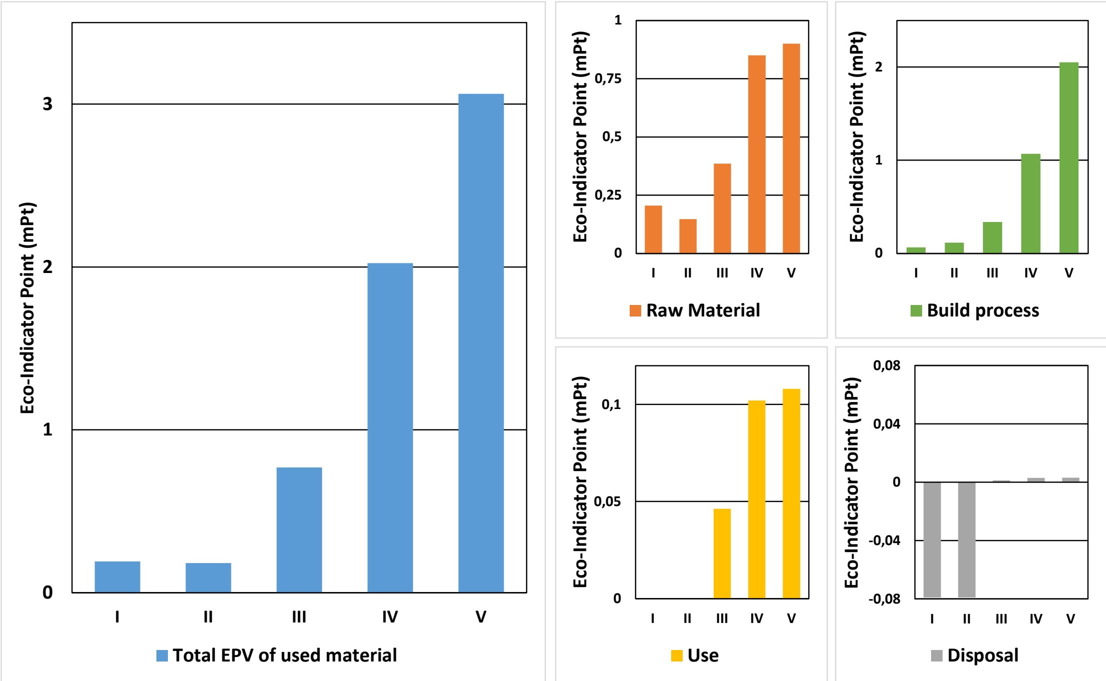

Figure 4 Illustration of samples' total EPV and distribution in life phases

The FDM samples have not only advantages in energy consumption during the build process, but also have low total life-cycle environmental impact in comparison to SLA and Polyjet printing. These advantages are mostly based on their high process overhead coefficient, recycling possibility and low material usage due to less than 25% infill. Especially the low infill density in FDM parts and the resultant reduction of the needed build material have contributed to the outstanding environmental performance: In view of total EPV per kilogram build material, the Polyjet samples IV and V are increased by factors of two and three compared with the FDM sample II. If the weights of used materials are taken into consideration, the factors expand to about 11 and 17 respectively. Moreover, according to the LCA calculation by Kreiger and Pearce [33], the ABS and PLA parts manufactured by personal FDM printers have already an advantage in terms of energy consumption and CO_2 emission in comparison to the conditional injection molded parts, if their infill is less than 79%, which is fulfilled in this research's samples. This whole discussion, however, does not take material strength and other mechanical properties into account.

4.2 Evaluation with focus on build process

A new approach was developed later by Bourhis et al. [44] using Eco-Indicator 99 [36] to comprehensively evaluate the environmental impact of AM processes. The sources of energy consumption in manufacturing processes are divided into three flows: electric consumption, material consumption and fluids consumption. In the final calculation, the electric consumption (in kWh), the material consumption (in kg) and the fluids consumption (in l) are converted into the environmental impact value (E.I.) with the same unit "mPt" as in Eco-Indicator 95. Due to a limited understanding of the energy consumption distribution in 3D printers, the following simplified equations are applied.

$$E.I._{sum} = E.I._{material} + E.I._{machine} \quad (11)$$

$$E.I._{material} = \sum_i m_{material_i} * f_{c_{material_i}} \quad (12)$$

$$E.I._{machine} = P_{machines} * f_{c_{electricity}} * t_{man} \quad (13)$$

$f_{c_{electricity}}$: Electricity factors (22 mPt/kWh) [50]

$f_{c_{material}}$: Material factors (mPt/kg) [50]

$m_{material_i}$: Weight of the material (g)

$P_{machines}$: Machine power (W)

t_{man}: Manufacturing time for a sample (s)

The entire composition of the calculation formula and its relevant parameters are shown in **Figure 5**.

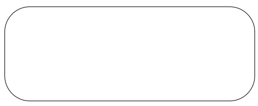

Figure 5 Process model for calculation of environmental impact in build process

The results of E.I. are summarized as following in **Table 6**.

Table 6 Environmental impact of samples calculated with Eco-Indicator 99

Sample	t_{man} (min)	$P_{machine}$ (W)	$E.I._{machine}$ (mPt)	$m_{material}$ [$m_{support}$](g)	$f_{c_{material}}$ (mPt/kg)	$E.I._{material}$ (mPt)	$E.I._{sum}$ (mPt)	$E.I._{sum}/m_{smp}$* (mPt/g)
I	62	100	2.27	15.8	630	9.954	12.23	0.803
II	63	150	3.47	15.8	400	6.32	9.79	0.956
III	380	60	8.36	38.52	510	19.65	28.01	0.965
IV	75	1500	41.25	51 [34]	510	43.35	84.60	2.972
V	144	1500	79.20	56 [34]	510	45.9	125.10	4.325

* See sample weights in **Table 2**

It can be seen from the table that the results correspond to those calculations with Eco-Indicator 95. Among the three AM processes FDM has the lowest, SLA medium and Polyjet printing the highest environmental impact.

4.3 Comparison of the results

In comparison with the method by Luo et al. [43], the approach by Bourhis et al. [44] has applied the newer Eco-Indicator 99 instead of Eco-Indicator 95, which is more accurate and most commonly used nowadays [44]. Furthermore, the approach has gone beyond the electrical consumption of the machine in process and achieved a complete analysis of the build process. However, without life cycle methodology as basis, the results from the approach by Bourhis et al. [44] are only comparable with results of life phases 1 and 2 by Luo et al. [43], and therefore are more suitable for identifying the results of changing part's design or process parameters in their corresponding final products' environmental impacts. In both analyses, the machine power has a large impact on the final assessment and should be studied further.

5. Study of surface roughness and sensory assessment

5.1 Sample roughness measurement

Instrument

A Surftest SJ-210 surface roughness tester from Mitutoyo was used for roughness measurements. The instrument works with a standard detector (measuring force 4 Nm and stylus 5 µmR/90̊) to measure surface roughness and topography. The detector has a vertical measure range of 360 µm and a vertical resolution of 0.02 µm.

Filter and sample length

Subjective roughness properties of surfaces are perceived by touching which includes finger pressure and positioning on the material surface. So far the research hypothesis is that the stimulus on the fingers can be compared with a vibration of a given frequency [18]. Any stimulus below the finger discriminative capacity is not detectable [21]. Therefore, the profiles detected by the profilometer must be filtered according to the human discriminative capacity for vibrotactile frequencies. According to Hollins et al. [19] the scanning velocity of the fingers is on average 90 mms^{-1} and to Ye et al. [20], the vibration is perceptible by fingers through vasoconstriction with a frequency greater than 63 Hz. Meanwhile, the discriminative capacity of human fingers equals the ratio of the scanning velocity and the frequency [21]. Therefore, the roughness profiles were filtered by Gaussian high-pass filter with a cutoff length[3] of 800 µm (0.03”) and evaluation length was chosen to be five times the sampling length[4] [27].

Evaluation area and number of acquisitions

Due to the 3D printed parts' inherent properties of anisotropic facets [30] and different surface quality of each facet [31], four roughness samples were collected on each acquisition area. The acquisition areas include top, front, side facets, TW and SU/SD geometric features (in Figure 1) for

[3] Cutoff λc: Cutoff length, as parameter used in profile filters, determines which wavelengths belong to roughness and which ones to waviness. Only the roughness parts will be used to calculate Ra, Rz etc.

[4] Sampling Length: Sampling Length is the reference length for roughness evaluation, whose length is equal to the cutoff length.

all five samples. Five surface roughness amplitude parameters, which are independent from each other, were calculated from the filtered profiles: Ra, Rq, Rz, Rsk, and Rku. Their definitions are listed in **Table 7**. The same parameters were used in studies [21] and [30].

Table 7 Definition of roughness parameters [27]

Symbol	**Name (unit)**	**Illustration**	**Definition**
Ra	Arithmetical average roughness (µm)	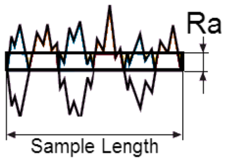	Arithmetic mean of the absolute values of the surface departures from the mean plane
Rq	Root mean squared (µm)	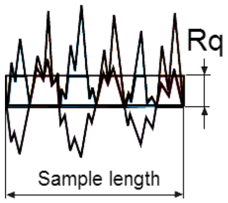	Geometric average value of the profile departure from the mean line within a sampling length
Rz	Maximum peak-to-valley height (µm)	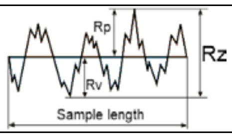	Maximum peak-to-valley height of the profile within the sampling length
Rsk	Topography height skewness distribution (–)	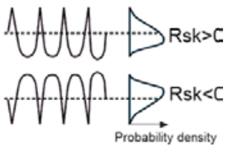	Measurement of the symmetry of the surface deviations about the mean reference plane. Rsk is negative if the distribution has a longer tail at the lower side of the mean plane and positive if the distribution has a longer tail at the upper side of the mean plane.
Rku	Kurtosis of the topography height distribution (–)	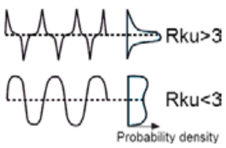	Measurement of the peak or sharpness of the surface height distribution. A spiky surface has a high Rku value and a bumpy surface has a low Rku value.

5.2 Sensory evaluation

The minimum number of persons for sensory evaluation (assessors), order of presentation, and number of samples are defined in standards by the Association Française de Normalisation (AFNOR) on sensory analysis of materials [24] [25].

Assessor (subject) selection

The purpose of the sensory analysis was to study the ranking and the perceptible differences between different samples with various surface qualities. According to SSHA [26], a minimum number of 20 assessors are required for the ranking test to be significant. A group of 32 assessors was recruited for sensory evaluation. All assessors are students at the University of California, Davis and possess sufficient English skills to complete the whole assessment. The group consisted of 25% students majoring in Arts and 75% in Science. 81.3% of the group had no previous experiences with 3D printing according to their own statement.

Experimental sessions

The experiments were held in spaces with sufficient illumination and the assessors performed the experiment one at a time. The time taken per evaluation was approximately 12 min and the full study was finished in 6 days. No monetary compensation was given to the assessors.

The whole experiment was arranged in three successive assessments (hedonic, tactile and visual) and the assessors were asked to rank the samples after touching and/or seeing all five samples for each assessment type. The partition of sessions and ranking methods are based on Ramananantoandro et al. [21]. As the assessors had not seen the samples beforehand, the assessments were conducted in the following order:

(1) Analysis of hedonic appreciation, i.e. ranking in order of personal preference of samples: rank 1 was assigned to the least appreciated sample and rank 5 to the most appreciated sample. There was no instruction on criterion of preference. The assessors did not see the samples during this session.

(2) Analysis of tactile roughness perception: a rank of 1 was assigned to the sample with the roughest surfaces and rank 5 to the sample with the smoothest surfaces. Also during this session, the assessors did not see the samples.

(3) Analysis of visual impression of roughness, without touching the samples: rank 1 was assigned to the sample with the roughest surfaces and rank 5 to the sample with the smoothest surfaces.

The hedonic and tactile sessions were conducted in a neutrally-colored cabinet, which has openings on both sides facing assessors and researchers. The opening facing the assessors was covered with a white curtain so that the perceived sample is invisible for assessors. The design is similar to Chen et al. [26].

During the experiments, assessors were allowed to retest to make sure of their ranking. They were allowed to use active dynamic touch to explore the samples and no restriction was given as to the number of hands used. The order of sample presentation to each assessor in each session was randomly arranged.

To avoid possible influence from sample color during the visual session, the experiment moderator emphasized before the session that the ranking should only be based on the samples' surface roughness, regardless of other surface features.

Agreement between the assessors

The sensory analysis was performed by Minitab® 17 software package. Kendall's coefficient of concordance (W) was calculated for each assessor as a measure of the amount of agreement between the ranks [28]. A value of W close to zero describes a discordance between the ranks of the variables, while a value close to 1 represents a perfect agreement between the ranks of the variables. The value of W was 0.10 and 0.33 for hedonic and tactile assessment, which indicates higher discrepancy among the various assessors. The value of W was 0.64 for visual assessment, which indicates a greater unanimity. The p-values (statistical hypothesis testing value) of the three assessment methods are 1.40E-02, 1.97E-08, 8.91E-17 respectively and < 0.05, which allows rejecting the null hypothesis that there was no agreement among the judges. Therefore, the agreement among assessors provides the basis for the following analysis.

Sensory analysis

The ranking of each assessor for each sample was decoded; the average score for each sample was calculated and summarized in **Figure 6**. The significance of observation is given at the 95%

confidence interval level.

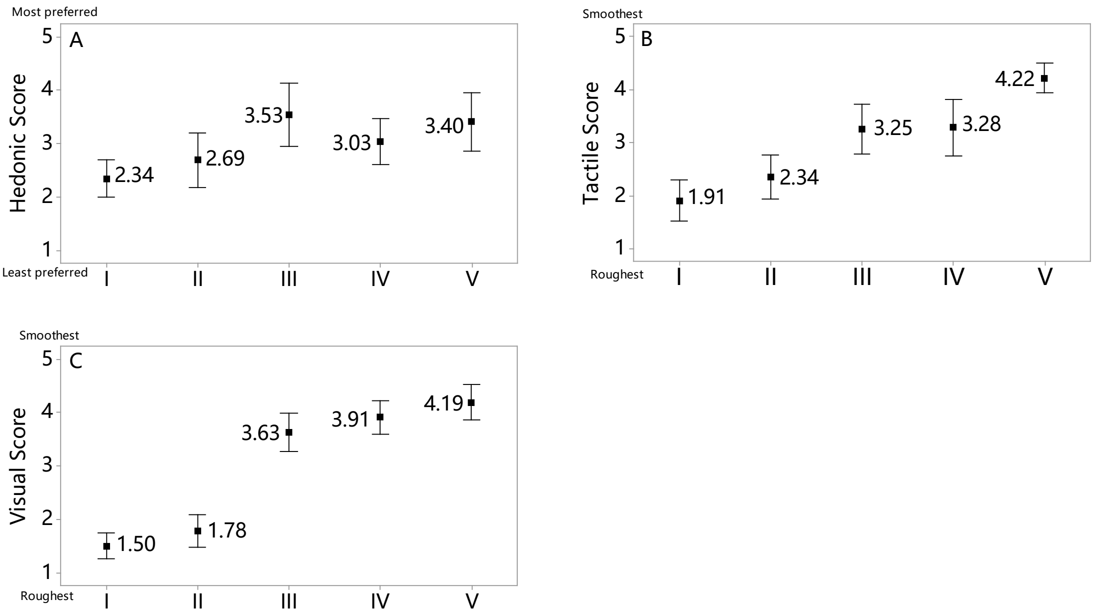

Figure 6 Ranking scores obtained from experimental sessions: (A) hedonic impression, (B) tactile and (C) visual assessments of surface roughness. Average and confidence interval 95% (n=32 assessors). Score 1 = the least preferred / roughest sample; 5 = the most preferred / smoothest sample.

For the hedonic appreciation (**Figure 6** (A)), two samples were preferred by the assessors. The sample with the highest hedonic score is manufactured with SLA (III). The worst are the samples manufactured with FDM (samples I and II). Although the PLA (I) and ABS (II) materials have close average scores, the ABS sample has a slightly wider confidence interval.

For the tactile assessment of surface roughness by active touch (**Figure 6** (B)), the assessors tended to have a clear distinction between the different samples. The ranking mirrors the expectation that a smaller layer thickness produces smoother surfaces. Samples with smaller layer thickness were assigned higher scores and the two FDM samples (I and II) were assessed to be the roughest. The Polyjet sample with Digital material (V) has the best ranking.

Concerning visual observation (**Figure 6** (C)), the samples tend to be distinguished significantly in two groups. While the FDM samples (I and II) have again the lowest scores, the SLA (III) and Polyjet samples (IV and V) have nearly the same scores. With the same judgment objective of surface roughness in tactile and visual sessions, the results can be interpreted in such a way that the assessors have a more realistic judgment in the tactile test than in the visual test, or the differences are not easily perceptible by eyes.

Except for the SLA sample (III), the average scores from the hedonic appreciation assessment (A) have the same pattern as the ranking in tactile roughness assessment (B). A possible explanation is that the surface roughness influences significantly the assessors' personal preference towards plastics parts and to prefer smoother surfaces to rougher ones. However, the amplitude between the lowest and highest average score in (A) is reduced by comparison to (B), which means that for individuals the surface roughness is only one aspect in personal preference. The slightly higher ranking of FDM samples (I and II) in hedonic appreciation assessment (A) compared to assessments

B and C could be attributed to their relatively light weight due to low infill density. The significantly higher average score and wider confidence interval for the SLA sample (III) indicates that its unique material per se was appreciated by a certain number of assessors.

Correlations between sensory analysis and roughness

The interrelation between sensory analysis and measured roughness was observed by means of linear regression analysis. Pearson's correlation coefficients [45] between the five roughness parameters and sensory average scores are presented in **Table 8**.

Table 8 Pearson's correlation coefficient (r) between sensory average score and roughness parameters (Significant correlations at 0.1 level are presented in bold.)

Roughness parameters	Hedonic	Tactile	Visual
Ra Arithmetical average roughness	-0.892	**-0.916**	**-0.978**
Rq Root mean squared	-0.888	**-0.917**	**-0.978**
Rz Maximum height	-0.881	**-0.931**	**-0.987**
Rsk Topography height skewness distribution	0.589	0.744	0.885
Rku Kurtosis of the topography height distribution	**0.914**	0.791	0.895

5.3 Results

Tactile and visual results

The common surface roughness parameters Ra, Rq, and Rz are negatively correlated with the tactile average score at the 0.1 level and more significantly with the visual average score at the 0.05 level. This result indicates that the surfaces perceived as rough by fingers and eyes have a high value of Ra, Rq, and Rz, among which Rz has the highest correlation.

The biplots of Rz versus tactile and visual average scores are represented in **Figure 7** (A) and (B) respectively, and the biplots of Ra versus tactile and visual average scores are presented in **Figure 8** (biplots of Rq have exact the same pattern). The higher correlation coefficient of Rz compared to Ra is reflected by the sample III's and IV's positions. In **Figure 7** (Rz), sample IV has smoother surfaces (low Rz value) than III and additionally also higher ranking scores. In **Figure 8**, sample III tends to have smoother surfaces (low Ra value) than IV.

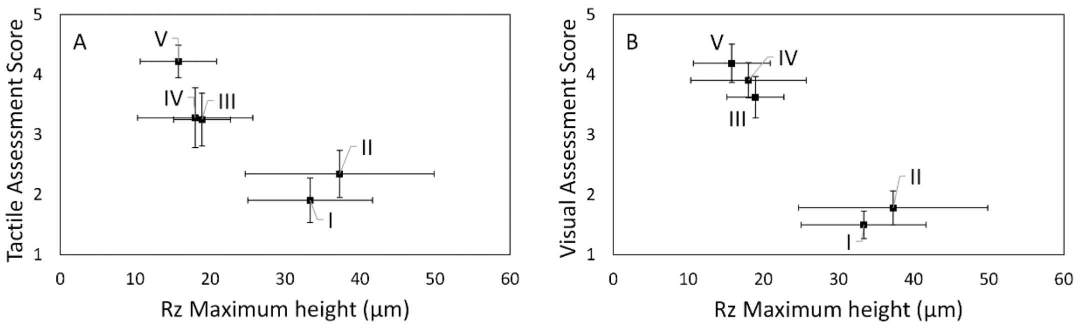

Figure 7 Biplots of tactile and visual assessment scores versus roughness parameter Rz. Average and confidence interval 95%. Score 1 = the roughest sample; 5 = the smoothest sample.

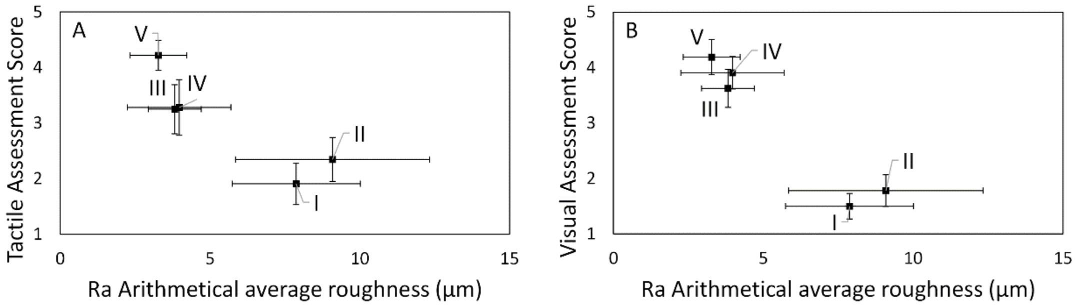

Figure 8 Biplots of tactile and visual assessment scores versus roughness parameter Ra. Average and confidence interval 95%. Score 1 = the roughest sample; 5 = the smoothest sample.

Rz represents both the tactile and visual roughness well. FDM samples with PLA and ABS (I and II) as build material were perceived differently by human touch and eyes. The ABS sample (II) has even a higher value of Rz than the PLA sample (I). In the tactile assessment this phenomenon might be attributed to the perception of extremely smooth surface when scanning along the texture of ABS sample, whose minimum value of Rz is 2.4 µm while minimum value of Rz on PLA sample is 4.11 µm. In the visual assessment the phenomenon may be attributed to the different colors of the build materials. As already researched by Whitaker et al. [34] and Klatzky and Lederman [35], the color texture influences roughness appreciation by the observers.

Aligned with the perceived ranking by human touch and observation, the Polyjet sample with Digital material (V) has the minimum average Rz value among all samples and also a small confidence interval. The average Rz values of Polyjet and SLA samples correspond to the general principles of these AM processes. In Polyjet printing and SLA an increase in layer thickness leads to increased surface roughness. The trend is perceptible in both tactile and visual assessments. The reasons for a more significant difference in visual assessment scores between translucent Polyjet and SLA samples may be also attributed to the obvious texture on the SLA sample (III).

In summary, Rz represents an overall significant measurement of the surface roughness on 3D printed parts, but only one parameter is not enough to comprehensively characterize tactile and visual human perception, as surface texture and material colors have also significant influence. However, this result is remarkable as Rz being not the most common parameter for surface roughness measurement of 3D printed parts. Ra, as the most commonly used measurement parameter is slightly inferior to Rz in reflection of human tactile and visual perception.

Hedonic results

For the hedonic assessment, there is a significant correlation between hedonic scores and Rku (Kurtosis of the topography height distribution) in **Figure 9**.

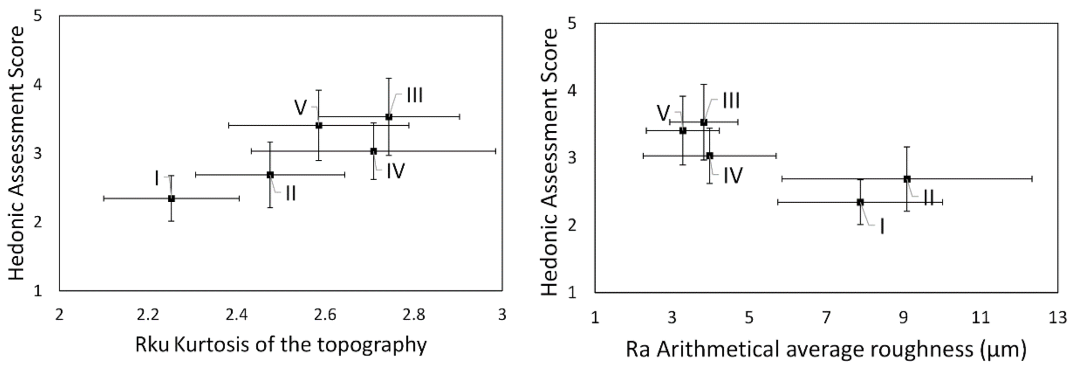

Figure 9 Biplot of hedonic assessment score versus roughness parameter Rku and Ra. Average and confidence interval 95%. Score 1 = the most preferred sample; 5 = the least preferred sample.

Rku has correctly predicted the average hedonic scores of 4 samples, except for the Polyjet sample (V). One reason might be that rugged and relative rough surfaces were not preferred by the assessors. In other words, samples with a low frequency of extreme peak or valley height around an average line are preferred to those with high frequency. In comparison, as roughness parameter with the second highest correlation, Ra has predicted the positions of three samples.

6. Conclusions

The research has focused on three important aspects of personal 3D printing processes, i.e. manufacturing cost, sustainability, and visuotactile perception of surface roughness.

For manufacturing cost, two main approaches by Hopkinson and Dickens [38] and Ruffo et al. [39] exist, which are applied to personal 3D printers with appropriate assumptions to the print scenario. In calculation with the benchmark samples, the Polyjet parts have the highest cost while the FDM parts have the lowest. With personal 3D printing's scenario of one single part being manufactured in a build, labor cost contributes greatly to manufacturing cost. With more than one parts manufactured in one build, the cost of Polyjet printing could be reduced.

In terms of environmental impact in life cycle, life cycle methodology and Eco-Indicator 95 are applied by Luo et al [43]. FDM products have the lowest environmental impact while Polyjet products the highest, which could be attributed to FDM's relatively low process energy consumption and the possibility to be recycled when the products are disposed. An infill density less than 100% is also a crucial factor. Another approach by Bourhis et al [44] focuses on the print process per se consumption with the more accurate Eco-Indicator 99. The electric, material and fluids consumption are in scope and analyzed separately during the print process. With this approach, FDM products have the lowest environmental impact while Polyjet parts have the highest. Fill ratio, density and part weight can be varied in FDM and change the impacts considerably.

This research has also investigated the sensory responses of 32 individual assessors of 3D printed part quality, and the variation and subjectivity of their assessments. The assessors were able to distinguish the differences of five samples of 3D printed parts with various build materials. Concerning the hedonic assessment, the assessors preferred smooth surfaces with a high Rku value. In contrast, the agreements between the assessors were low by comparison to tactile and visual assessments, which indicate assessors' various preference towards 3D printed parts.

The measured 2D surface roughness parameters have a significant correlation with the sensorial ranking scores. The parameter Rz (Maximum peak-to-valley height) was superior to Ra and Rq, which are the most commonly used surface roughness parameters. Rz has a higher correlation with the tactile assessment results and an even better fit with the visual assessment scores. However, the sensory judgments are also subjected to other influencing factors, e.g. surface texture and build material color. Therefore, Rz alone cannot comprehensively characterize different human perception among samples.

Overall, the Polyjet samples have achieved the best rankings in all hedonic, tactile and visual assessments, but also have the highest manufacturing costs and environmental impact. The SLA sample has a middle ranking in tactile and visual assessments, but its unique material per se was significantly more appreciated in hedonic sensation. While the FDM samples have the worst overall ranking, they were manufactured with the lowest costs and environmental impact. Their light weight due to low infill density contributes not only to assessors' hedonic appreciation, but also significantly to sustainability [33]. In conclusion, the three investigated AM processes for personal 3D printers have their own advantages and disadvantages. The different aspects of costs, environmental impact and quality have to be weighed against each other. Cost-benefit analysis has proven to be one simple and transparent method to combine different sustainability dimensions [48]. However, it could be concluded from this research's results that the samples with best surface quality are also accompanied with highest manufacturing cost and environmental impacts. Further research should study the subjective assessment in more detail. If specific applications for the printed parts are given that exceed aesthetics, material properties should be taken into account. Furthermore, different AM processes have advantages in printing specific shapes and materials which can be investigated further in future in connection with the consumer wishes.

Acknowledgments: We thank the UC Davis students for help with collecting data for sensory analysis and Steven Lucero in the TEAM Lab for manufacturing the samples. The authors are also thankful for the funding through the Undergraduate Research Opportunities-Program (UROP) of RWTH Aachen University.

7. References

[1] Wohlers, T., 2014, Wohlers report 2014, Wohlers Associates, Fort Collins, Col.

[2] Stratasys, 'FDM Technology: 3D print durable parts with real thermoplastic' [Online]. Available: http://www.stratasys.com/3d-printers/technologies/fdm-technology. [Accessed: 12- Feb- 2015].

[3] RepRap, 'RepRap' [Online]. Available: http://reprap.org/. [Accessed: 12- Feb- 2015].

[4] ISO/ASTM 52900:2015, 2015, Additive Manufacturing – General Principles – Terminology, norm, Switzerland.

[5] 3D Hubs, 2015, '3D Printing Trends January 2015' [Online]. Available: https://www.3dhubs.com/trends. [Accessed: 12- Feb- 2015].

[6] Nancharaiah, T., Ranga Raju, D., and Ramachandra Raju, V., 2010, 'An experimental investigation on surface quality and dimensional accuracy of FDM components', International Journal on Emerging Technologies, 1(2), pp. 106-111.

[7] Williams, R., Komaragiri, S., Melton, V., and Bishu, R., 1996, 'Investigation of the effect of various build methods on the performance of rapid prototyping (stereolithography)', Journal of Materials Processing Technology, 61(1-2), pp. 173-178.

[8] Kechagias, J., Iakovakis, V., Giorgo, E., Stavropoulos, P., Koutsomichalis, A., and Vaxevanidis, N., 2014, 'Surface roughness optimization of prototypes produced by Polyjet direct 3d printing technology', Proceedings of the 1st International Conference on Engineering and Applied Sciences Optimization, Kos Island, pp. 2877-2888.

[9] Kim, G., and Oh, Y., 2008, 'A benchmark study on rapid prototyping processes and machines: quantitative comparisons of mechanical properties, accuracy, roughness, speed, and material cost', Proceedings of the Institution of Mechanical Engineers, Part B: Journal of Engineering Manufacture, 222(2), pp. 201-215.

[10] Mahesh, M., Wong, Y., Fuh, J., and Loh, H., 2004, 'Benchmarking for comparative evaluation of RP systems and processes', Rapid Prototyping Journal, 10(2), pp. 123-135.

[11] Makerbot, 2015, 'PLA TECHNICAL SPECIFICATIONS' [Online]. Available: http://store.makerbot.com/filament/pla#. [Accessed: 23- Feb- 2015].

[12] Makerbot, 2015, 'ABS TECHNICAL SPECIFICATIONS' [Online]. Available: http://store.makerbot.com/filament/abs. [Accessed: 23- Feb- 2015].

[13] Formlabs, 2015, 'Clear Photopolymer Resin for Form 1+ Material Properties' [Online]. Available: http://formlabs.com/media/upload/Clear-DataSheet.pdf. [Accessed: 23- Feb- 2015].

[14] Stratasys, 2015, 'PolyJet™ Materials Data Sheet' [Online]. Available: http://www.stratasys.com/~/media/Main/Secure/Material%20Specs%20MS/PolyJet-Material-Specs/PolyJet_Materials_Data_Sheet.pdf. [Accessed: 23- Feb- 2015].

[15] Stratasys, 2015, 'Digital Materials Data Sheet' [Online]. Available: http://www.stratasys.com/~/media/Main/Secure/Material%20Specs%20MS/PolyJet-Material-Specs/Digital_Materials_Datasheet.pdf. [Accessed: 23- Feb- 2015].

[16] Stratasys, 2015, 'PolyJet Digital Materials' [Online]. Available: http://www.stratasys.com/materials/polyjet/digital-materials. [Accessed: 25- Feb- 2015].

[17] Wohlers, T., 2014, Wohlers report 2014, Wohlers Associates, Fort Collins, Col.

[18] Lederman, S., 1974, 'Tactile roughness of grooved surfaces: The touching process and effects

of macro- and microsurface structure', Perception & Psychophysics, 16(2), pp. 385-395.
[19] Hollins, M., Bensmaïa, S., and Roy, E., 2002, 'Vibrotaction and texture perception', Behavioural Brain Research, 135(1-2), pp. 51-56.
[20] Ye, Y., and Griffin, M., 2014, 'Relation between vibrotactile perception thresholds and reductions in finger blood flow induced by vibration of the hand at frequencies in the range 8–250 Hz', Eur J Appl Physiol, 114(8), pp. 1591-1603.
[21] Ramananantoandro, T., Larricq, P., and Eterradossi, O., 2014, 'Relationships between 3D roughness parameters and visuotactile perception of surfaces of maritime pinewood and MDF', Holzforschung, 68(1).
[22] Baumers, M., Tuck, C., Wildman, R., Ashcroft, I., and Hague, R., 2015, 'Energy inputs to additive manufacturing: does capacity utilization matter?', EOS, 1000(270), pp. 30-40.
[23] BP X10-040, Caractérisation sensorielle des matériaux - Méthodologie générale - Recommandations méthodologiques pour l'analyse sensorielle de la matière première au produit fini (AFNOR, 2003)
[24] BP X10-041, Caractérisation sensorielle des matériaux - Recommandations pratiques pour l'analyse tactile de la matière première au produit fini (AFNOR, 2004)
[25] Depledt, F., and Strigler, F., 2009, Évaluation sensorielle (3e éd.) :Manuel méthodologique - retirage broché , Tec & doc, Paris.
[26] Chen, X., Shao, F., Barnes, C., Childs, T., and Henson, B., 2009, 'Exploring relationships between touch perception and surface physical properties', International Journal of Design, 3(2), pp. 67-76.
[27] Czichos, H., Saito, T., and Smith, L., 2006, Springer handbook of materials measurement methods, Springer, [Germany].
[28] Oger, R., and Saporta, G., 1991, 'Probabilites, Analyse des Donnees et Statistique.', Biometrics, 47(2), p. 783.
[29] Ruffo, M., Tuck, C., and Hague, R., 2007, 'Make or buy analysis for rapid manufacturing', Rapid Prototyping Journal, 13(1), pp. 23-29.
[30] Dezső, G., and Kósa, P., 2013, 'Roughness of plane faces produced by additive manufacturing', Electronic Journal of Environmental Sciences, 6, p. 181.
[31] Byun, H., and Lee, K., 2006, 'Determination of the optimal build direction for different rapid prototyping processes using multi-criterion decision making', Robotics and Computer-Integrated Manufacturing, 22(1), pp. 69-80.
[32] Sreenivasan, R., Goel, A., and Bourell, D., 2010, 'Sustainability issues in laser-based additive manufacturing', Physics Procedia, 5, pp. 81-90.
[33] Kreiger, M., and Pearce, J., 2013, 'Environmental Life Cycle Analysis of Distributed Three-Dimensional Printing and Conventional Manufacturing of Polymer Products', ACS Sustainable Chem. Eng., 1(12), pp. 1511-1519.
[34] Whitaker, T., Simões-Franklin, C., and Newell, F., 2008, 'Vision and touch: Independent or integrated systems for the perception of texture?', Brain Research, 1242, pp. 59-72.
[35] Klatzky, R.L., and Lederman, S.J., 2010, 'Multisensory texture perception', Multisensory object perception in the primate brain, Springer, New York, pp. 210-230.
[36] Pre-sustainability.com, 1999, 'Eco-indicator 99 Manual for Designers' [Online]. Available: http://www.pre-sustainability.com/download/EI99_Manual.pdf. [Accessed: 20- Mar- 2015].
[37] SON, Y., 1991, 'A cost estimation model for advanced manufacturing systems', International

Journal of Production Research, 29(3), pp. 441-452.
[38] Hopkinson, N., and Dicknes, P., 2003, 'Analysis of rapid manufacturing—using layer manufacturing processes for production', Proceedings of the Institution of Mechanical Engineers, Part C: Journal of Mechanical Engineering Science, 217(1), pp. 31-39.
[39] Ruffo, M., Tuck, C., and Hague, R., 2006, 'Cost estimation for rapid manufacturing - laser sintering production for low to medium volumes', Proceedings of the Institution of Mechanical Engineers, Part B: Journal of Engineering Manufacture, 220(9), pp. 1417-1427.
[40] CareerBliss, 2015, 'UC Davis Lab Technician Salaries' [Online]. Available: http://www.careerbliss.com/uc-davis/salaries/lab-technician/. [Accessed: 19- Mar- 2015].
[41] Localwiki.org, 2015, 'PG&E - Davis' [Online]. Available: https://localwiki.org/davis/PG%26E. [Accessed: 19- Mar- 2015].
[42] Thomas, D., and Gilbert, S., 2014, Costs and Cost Effectiveness of Additive Manufacturing, National Institute of Standards and Technology, U.S. Department of Commerce.
[43] Luo, Y., Ji, Z., Leu, M., and Caudill, R., 1999, 'Environmental performance analysis of solid freedom fabrication processes', Proceedings of the 1999 IEEE International Symposium, pp. 1-6.
[44] Bourhis, F., Kerbrat, O., Hascoet, J., and Mognol, P., 2013, 'Sustainable manufacturing: evaluation and modeling of environmental impacts in additive manufacturing', Int J Adv Manuf Technol, 69(9-12), pp. 1927-1939.
[45] Salkind, D., 2006, Encyclopedia of Measurement and Statistics, SAGE Publications, Thousand Oaks.
[46] Pre-sustainability.com, 1995, 'The Eco-indicator 95' [Online]. Available: http://www.pre-sustainability.com/download/EI95FinalReport.pdf. [Accessed: 20- Mar- 2015].
[47] Stratasys.com, 2015, 'What is FDM Technology' [Online]. Available: http://www.stratasys.com/3d-printers/technologies/fdm-technology/faqs. [Accessed: 06- May- 2015].
[48] Linke, B., Corman, G., Dornfeld, D., and Tönissen, S., 2013, 'Sustainability indicators for discrete manufacturing processes applied to grinding technology', Journal of Manufacturing Systems, 32(4), pp. 556-563.
[49] Serres, N., Tidu, D., Sankare, S., and Hlawka, F., 2011, 'Environmental comparison of MESO-CLAD® process and conventional machining implementing life cycle assessment', Journal of Cleaner Production, 19(9-10), pp. 1117-1124.
[50] Pre-sustainability.com, 1999, 'Eco-indicator 99' [Online]. Available: http://www.pre-sustainability.com/download/EI99_Manual.pdf. [Accessed: 14- May- 2015].
[51] Gibson, I., 2005, Advanced manufacturing technology for medical applications, J. Wiley, Chichester, West Sussex, England.
[52] Stratasys.com, 2015, 'PolyJet Technology' [Online]. Available: http://www.stratasys.com/3d-printers/technologies/polyjet-technology. [Accessed: 15- Jul- 2015].
[53] Malone, E. and Lipson, H., 2007, "Fab@Home: the personal desktop fabricator kit", Rapid Prototyping Journal, 13(4), pp. 245-255.